TUNABLE PHOTONIC BAND GAP IN A DOPED SEMICONDUCTOR PHOTONIC CRYSTAL IN NEAR INFRARED REGION

C.-J. Wu and Y.-C. Hsieh

Institute of Electro-Optical Science and Technology
National Taiwan Normal University, Taipei 116, Taiwan

H.-T. Hsu

Department of Communication Engineering
Yuan-Ze University, Chungli 320, Taiwan

Abstract—In this work, we theoretically investigate the tunable photonic band gap (PBG) in a semiconductor-dielectric photonic crystal made of highly doped n-type silicon (Si) layers alternating with silicon oxide layers. The tunable characteristic is studied by changing the donor impurity concentration in Si layer. The PBG is numerically analyzed in the near infrared frequency region from the reflectance calculated by the transfer matrix method. The effect of filling factor in Si layer on the photonic band gap is also illustrated. These tunable properties in such a photonic crystal provide some information that could be of technical use to the semiconductor optoelectronics, especially in communication applications.

1. INTRODUCTION

The field of photonic crystals (PCs), artificially periodic structures, was initialized during the late 1980s after the pioneering works by John and Yablonovitch [1–3]. The term "crystal" is used because the lattice constant (the spatial periodicity) of a PC is comparable to the wavelength of an electromagnetic wave. With the structurally periodic arrangement, the appearance of photonic band gap (PBG) structure in the dispersion relation is thus expected, and, in fact, the existence of PBG has been recognized as the most fundamental property for PCs.

One of the most promising applications in PCs is to engineer PBGs. PBGs, which are analogous to the electronic band gaps in solids, are frequency intervals in which electromagnetic waves are prohibited to propagate through the PCs because the waves are evanescent and will exponentially be attenuated. The direct consequences of PBGs include the total reflection of electromagnetic waves and the suppression of emission in PCs [4]. PCs with wide PBGs have proven to be of practical and experimental use in modern optical and photonic applications [5–10].

In addition to the need of wide band gaps in PCs, the feature of a tunable PBG attracts much attention in recent years. The PBG can be tuned by means of some external agents. For instance, it can be changed by the operating temperature and we call it the T-tuning. A superconductor/dielectric PC belongs to this type because of the temperature-dependent London penetration length in the superconducting materials [11–18]. Using a liquid crystal as one of the constituents in a PC, the T-tuning optical response is also obtainable [19–21]. Tuning in PBG can also be achieved by the external electric field and it is referred to as the E-tuning. PCs containing a ferroelectric material [22] or a liquid crystal [19–21] are good candidates for the E-tuning devices. Another called the M-tuning, which makes use of the magnetic field to tune the optical properties in a photonic crystal, is also available now [23–26].

Recently, PCs containing the semiconductor as one of the constituents have also been of interest to the photonic community. PCs with intrinsic semiconductor belong to T-tuning devices because the dielectric constant and the intrinsic carrier concentration of an intrinsic semiconductor are strongly dependent on temperature [27, 28]. PCs infiltrated with intrinsic semiconductor such as InSb are M-tuning devices [23, 29–31]. In addition, if the extrinsic doped semiconductor is incorporated in PCs, then optical response will be tuned directly by the doping concentration. In this case, it is known as the N-tuning (N is the carrier concentration) [32]. The N-tuning can switch the high reflectance range in a semiconductor-based PC, which is could be a positive impact on the semiconductor optoelectronics.
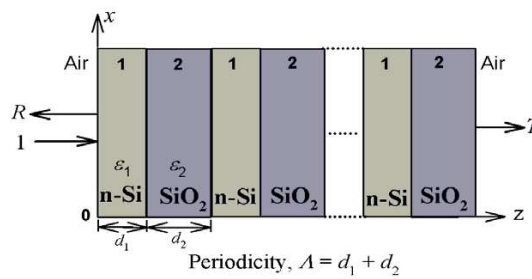
The purpose of this paper is to investigate the photonic band structure (PBS) in an n-Si/SiO$_2$ one-dimensional PC, in which n-Si is n-type silicon with highly doping donor impurities. We use the reflectance to analyze the PBS in the near infrared (IR) frequency region, 0.75–$3.0\,\mu$m. This region is of technical use to the optical communication and the telecommunication as well. The reflectance is calculated by making use of the transfer matrix method (TMM) [33]. We first investigate the reflectance as a function of impurity donor

concentration. It is found that high-reflectance can be obtained at a threshold concentration. In the wavelength-dependent reflectance, multiple PBGs can be produced at a larger spatial periodicity. The positions of PBGs will be shifted to the shorter wavelength as the doping concentration increases. Moreover, the widths of PBGs are strongly affected by the doping concentration. Additionally, the investigation of Si-layer filling factor on the PBGs will also be given.

2. BASIC EQUATIONS

In what follows, we shall calculate the reflectance for a one-dimensional n-Si/SiO$_2$ photonic crystal shown in Fig. 1. Here, we assume that the total number of periods is N_p and the total length of the structure is $N_p\Lambda$, where the spatial periodicity is equal to $\Lambda = d_1 + d_2$, where d_1 and d_2 are the thicknesses of layers n-Si and SiO$_2$, respectively. The optical properties in a PC are related to the refractive indices of the constituent layers, which are determined by the corresponding relative permittivities, i.e., $n_i = \sqrt{\varepsilon_i}$, where ε_i ($i = 1$ and 2). For SiO$_2$ in near IR, ε_2 is taken to be a constant, i.e., $n_2 = \sqrt{\varepsilon_2} = 1.5$ [34]. For n-Si, the relative permittivity, based on the plasma model, can be expressed as [32]

$$\varepsilon_1\left(\omega\right) = \varepsilon_\infty \left[1 - \frac{\omega_{pe}^2}{\omega^2 - j\omega\gamma_e} - \frac{\omega_{ph}^2}{\omega^2 - j\omega\gamma_h} \right], \qquad (1)$$

Figure 1. A one-dimensional n-Si/SiO$_2$ photonic crystal, in which doped n-type semiconductor n-Si with thickness d_1 occupies the region 1 and the dielectric SiO$_2$ with thickness d_2 is in the layer 2, respectively. The spatial periodicity is denoted by $\Lambda = d_1 + d_2$. The optical wave with a unit power in launched normally at the plane boundary of $z = 0$. The reflectance and transmittance are denoted by R and T, respectively.

where ε_∞ is the high-frequency limit of the relative permittivity, γ_e and γ_h are respectively the damping frequencies for the electrons and holes, and ω_{pe}, ω_{ph} are the electron and hole plasma frequencies given by

$$\omega_{pe,h} = \left(\frac{n_{e,h}e^2}{m_{e,h}\varepsilon_0} \right)^{1/2}. \tag{2}$$

Here, $m_{e,h}$ are the effective masses of electron and hole, $n_{e,h}$ are the electron concentration in the conduction band and the hole concentration in the valence band. The concentrations can be determined from the conservation of charge and they are given by

$$n_{e,h} = \sqrt{n_i^2 + \frac{N^2}{4}} \pm \frac{N}{2}, \tag{3}$$

where n_i is the intrinsic electron concentration of Si and N is the doping donor impurity concentration. It is worth mentioning that expression for Eq. (1) is based on the use of the temporal part $\exp(j\omega t)$ for all fields. It is also worth mentioning that the dielectric function in Eq. (1) does not include the optical process such as the interband transition. This assumption is physically reasonable in the near infrared region, especially at wavelengths near $1.5\,\mu$m which are widely applied in the optical communications. At this wavelength the photon energy is smaller than the gap energy of Si ($1.12\,$eV at room temperature) and therefore the optical process of interband transition will not be allowed to happen.

In this work, optical response such as the reflectance is used to study the PBG structure of the one-dimensional n-Si/SiO$_2$ photonic crystal. We employ the transfer matrix method (TMM) [33] to calculate the reflectance. According to TMM, expression for the reflectance R is given by

$$R = |r|^2 = \left| \frac{M_{21}}{M_{11}} \right|^2, \tag{4}$$

where r is the reflection coefficient, and M_{11}, M_{21} are the two matrix elements of the following total system matrix

$$\begin{pmatrix} M_{11} & M_{12} \\ M_{21} & M_{22} \end{pmatrix} = D_0^{-1} \left(D_1 P_1 D_1^{-1} D_2 P_2 D_2^{-1} \right)^{N_p} D_0. \tag{5}$$

Here, P_i ($i = 1, 2$) is the propagation matrix in layer i given by

$$P_i = \begin{pmatrix} \exp(jk_i d_i) & 0 \\ 0 & \exp(-jk_i d_i) \end{pmatrix}, \tag{6}$$

where $k_i = \omega c / \sqrt{\varepsilon_i}$ is the wave number in layer i, and D_q ($q = 0, 1, 2$) is the dynamical matrix in medium q which is written by

$$D_q = \begin{pmatrix} 1 & 1 \\ \sqrt{\varepsilon_q} & -\sqrt{\varepsilon_q} \end{pmatrix}, \tag{7}$$

where $q = 0$ is for the air with $\varepsilon_0 = 1$.

In addition to using the reflectance to study the optical properties, a direct calculation of photonic band structure (PBS) is of help to the study of PBGs. The PBS can be computed based on the following equation [33],

$$\cos(K\Lambda) = \cos(k_1 d_1) \cos(k_2 d_2) - \frac{1}{2}\left(\frac{n_1}{n_2} + \frac{n_2}{n_1}\right) \sin(k_1 d_1) \sin(k_2 d_2), \tag{8}$$

where the Bloch wave number is defined as $K = K_r - jK_i$. In the PBGs (stop bands), solution for K will have an imaginary part K_i so that the Bloch wave is evanescent. In the passband, where the Bloch wave can propagate through the PC, the solution for K is purely real, i.e., $K = K_r$.

3. NUMERICAL RESULTS AND DISCUSSION

In Fig. 2, we plot the relative permittivity of n-Si (Eq. (1)) for different donor impurity concentrations of $N = 1 \times 10^{19}$, 5×10^{19}, 10×10^{19}, and $20 \times 10^{19}\,\text{cm}^{-3}$ in the absence of damping frequencies, $\gamma_e = \gamma_h = 0$. We have taken the concentration to be on the order of $10^{19}\,\text{cm}^{-3}$ because such a high concentration is a necessary condition for the
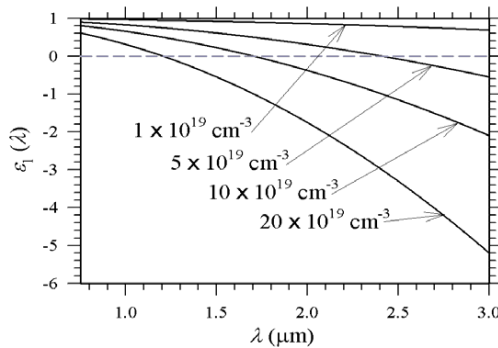

Figure 2. The relative permittivity of n-Si versus wavelength for different doping impurity concentrations of $N = 1 \times 10^{19}$, 5×10^{19}, 10×10^{19}, and $20 \times 10^{19}\,\text{cm}^{-3}$ in the case of zero damping frequencies $\gamma_e = \gamma_h = 0$.

purpose of achieving a sensitive tuning in near IR [32]. The other material parameters used in our calculation are $n_i = 1.02 \times 10^{10}\,\text{cm}^{-3}$, $\varepsilon_\infty = 1$, $m_e = 0.26m_0$, $m_h = 0.69m_0$, where $m_0 = 9.1 \times 10^{-31}\,\text{Kg}$ is the mass of free electron. Here, the zero permittivity is indicated by the dashed horizontal line below which the negative permittivity can be obtained. For $N = 1 \times 10^{19}\,\text{cm}^{-3}$, the overall values of permittivity are positive and smaller than one, falling in the range of $0.6 < \varepsilon_1 \leq 1$. At $N = 5 \times 10^{19}\,\text{cm}^{-3}$, the permittivity will be negative when $\lambda > 2.4\,\mu\text{m}$. The range of negative permittivity becomes large in the strongly doped n-Si such as $N = 20 \times 10^{19}\,\text{cm}^{-3}$. The existence of negative permittivity in n-Si makes it behave effectively as a metal at low frequencies.

In Fig. 3, we plot the reflectance and PBS of an n-Si/SiO2 PC as a function of the doping concentration at different filling factors of $f = d_1/\Lambda = 1/2$, $1/3$, and $1/4$, respectively. Here, the number of periods $N_p = 50$, and two different spatial periodicities, $\Lambda = 0.73\,\mu\text{m}$ (top panel) and $1.46\,\mu\text{m}$ (bottom panel), are taken. It is of interest to see that, in order to have $R = 1$, there exists a threshold value N_{th} in the doping concentration (marked by P_1, P_2, and P_3, respectively). The value of N_{th} increases with the decrease in f-value. In the upper panel, the values of N_{th} are $2.1 \times 10^{19}\,\text{cm}^{-3}$ ($f = 1/2$), $9.3 \times 10^{19}\,\text{cm}^{-3}$ ($f = 1/3$), and $17.5 \times 10^{19}\,\text{cm}^{-3}$ ($f = 1/4$). The corresponding PBS is plotted in the middle panel, in which the upper three blue curves indicate the calculated K_r's whereas K_i's are the lower red ones. Good agreement between the top and middle panels is seen. The value of N_{th} for each f-value is indicated by the vertical dash line. The region of PBG in the top panel is reflected by the existence of K_i's in the middle panel. In the lower panel, the values of N_{th} are $4.6 \times 10^{19}\,\text{cm}^{-3}$ ($f = 1/2$), $9.4 \times 10^{19}\,\text{cm}^{-3}$ ($f = 1/3$), and $17.9 \times 10^{19}\,\text{cm}^{-3}$ ($f = 1/4$). It can be seen from Fig. 3 that the variation in N_{th} is sensitive at $f = 1/2$, but insensitive for $f = 1/3$ and $1/4$.

The wavelength-dependent reflectance R at $\Lambda = 0.73\,\mu\text{m}$, $f = 1/2$, and $N_p = 50$ for different values of N is plotted in Fig. 4. For $N = 1 \times 10^{19}$, 5×10^{19}, and $10 \times 10^{19}\,\text{cm}^{-3}$, there are two PBGs. The first PBG with a narrow bandwidth is located below $1.0\,\mu\text{m}$. The other with a wider bandwidth has a right band edge near $2.0\,\mu\text{m}$. Both two gaps are enhanced and, in the meantime, are shifted to the left as N increases. However, the enhancement in the first PBG is much weaker than the second one. In addition, we see that the left band edge of the second PBG is strongly dependent on N. For $N = 20 \times 10^{19}\,\text{cm}^{-3}$, a third PBG emerges with the left band edge near $2.5\,\mu\text{m}$, leading to a three-gap structure in near IR. The calculated photonic band structures are plotted in Fig. 5. Excellent agreement is obtained as compared with Fig. 4.
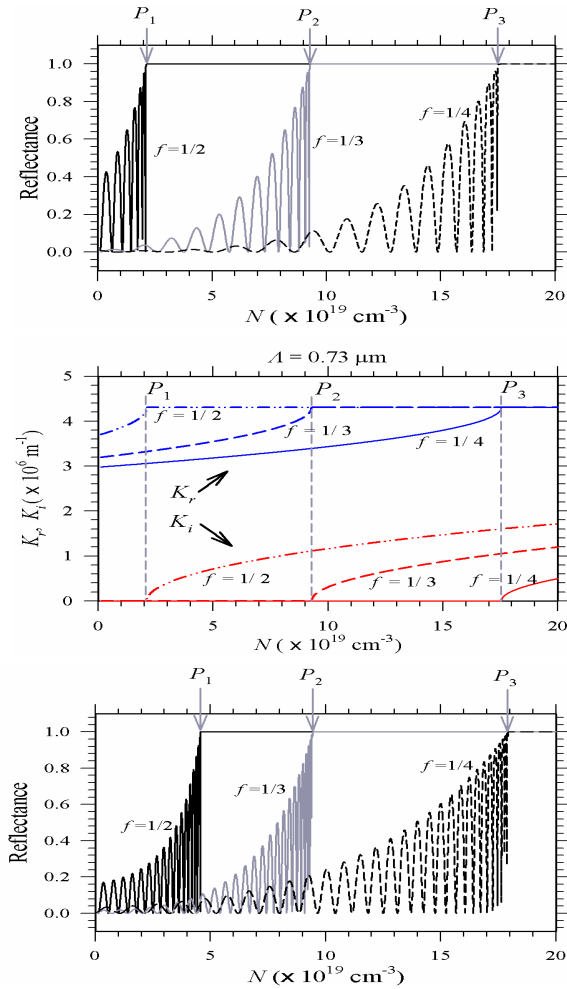
Figure 3. The calculated reflectance as a function of the doping concentration for the spatial periodicity $\Lambda = 0.73\,\mu$m (upper panel) and $1.46\,\mu$m (lower panel) at a fixed wavelength of $1.54\,\mu$m. Here, $N_p = 50$ is used.

If we double the spatial periodicity, i.e., $\Lambda = 1.46\,\mu$m and other conditions remain unchanged. The reflectance is now depicted in Fig. 6. It can be seen that the number of PBGs apparently increases. In this case, we have a four-gap structure, as numbered as 1–4. The bandwidth of gap 1 nearly unchanged as N changes, but an appreciable shift is seen. The change in gap 2 is not monotonic. The gap size first decreases
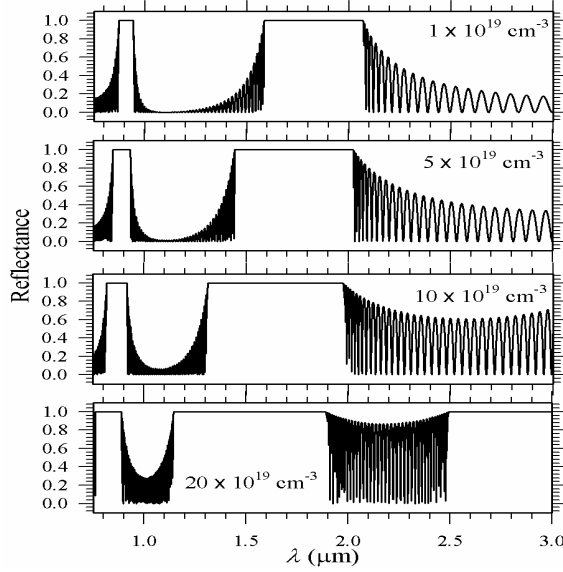
Figure 4. The calculated wavelength-dependent reflectance at four different doping concentrations at $\Lambda = 0.73\,\mu$m, $f = 1/2$, and $N_p = 50$. Two-gap structure is seen for $N = 1\times10^{19}$, 5×10^{19}, and $10\times10^{19}\,\text{cm}^{-3}$, but three gaps are obtained at $20 \times 10^{19}\,\text{cm}^{-3}$.
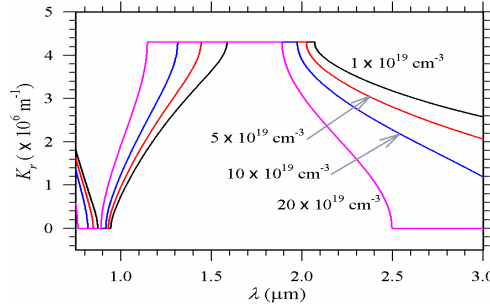

Figure 5. The calculated PBS at the same conditions used in Fig. 4. The horizontal parts represent the PBGs. The results are in good agreement with those in Fig. 4.

from $N = 1\times10^{19}$ to $10\times10^{19}\,\text{cm}^{-3}$, and then increases as N increases. As for gaps 3 and 4, their bandwidths are widened significantly as N increases. The enhancement in the gap 4 is much more pronounced.

When the doping concentration is strongest $(20 \times 10^{19}\,\mathrm{cm}^{-3})$, the reflectance becomes close to unity for a continuous and broad range of frequencies. Such a result arises from the metallic characteristic of Si, as mentioned previously in Fig. 2. A metal-dielectric PC is known to have a wider PBG compared with a dielectric-dielectric PC. It can be concluded from Figs. 4–6 that the number of PBGs strongly relies on doping concentration of Si and the physical size of the PC.

Figure 7 depicts the wavelength-dependent reflectance for four different filling factors at $N = 1 \times 10^{19}\,\mathrm{cm}^{-3}$ and $\Lambda = 0.73\,\mu\mathrm{m}$. It is seen that the bandwidth of the first gap decreases as f increases. The flat-top high-reflectance disappears at $f = 0.6$. After that the first gap re-opens, as illustrated at $f = 0.75$. On the other hand, the second gap has a maximum bandwidth at $f = 1/2$. Moreover, the shifting feature preserves, moving to the right as f decreases.
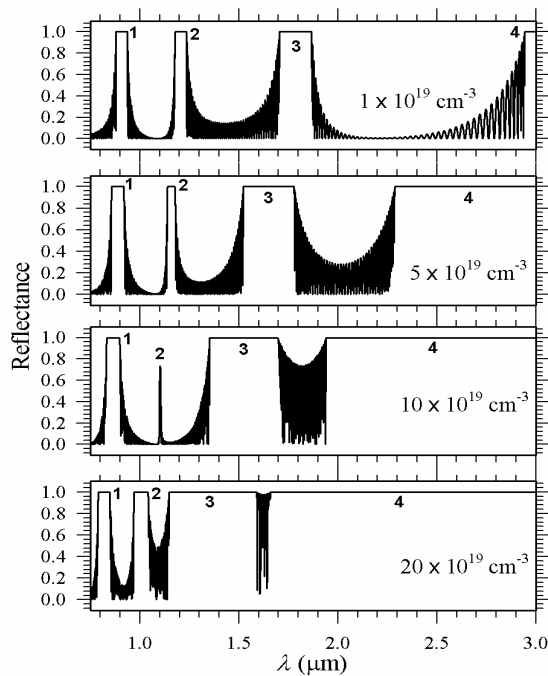
Figure 6. The calculated wavelength-dependent reflectance at four different doping concentrations at $\Lambda = 1.46\,\mu\mathrm{m}$, $f = 1/2$ and $N_p = 50$. There are four PBGs in the near IR.
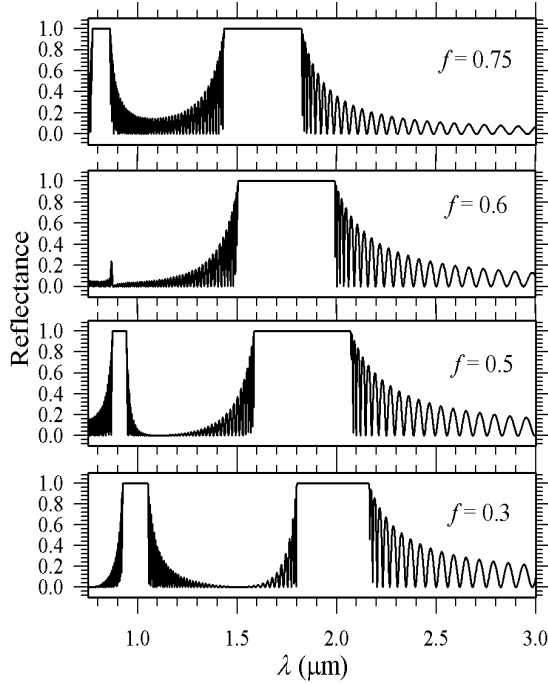
Figure 7. The calculated wavelength-dependent reflectance at four different filling factors of f = 0.75, 0.6, 0.5, and 0.3. Here, at $\Lambda = 0.73\,\mu m$, $N = 1 \times 10^{19}\,cm^{-3}$ and $N_p = 50$.

4. CONCLUSION

The photonic band structure in near IR region for an n-Si/SiO2 photonic crystal has been theoretically investigated. Due to the strong dispersion in the permittivity of n-Si semiconductor, the dependence of doping donor concentration has been illustrated in this work. Based on the numerical results, we draw the conclusions as follows: In the reflectance-versus-concentration plot, at a fixed wavelength of 1.54 µm, there is a threshold concentration N_{th} to achieve the high reflectance. The value in N_{th} increases as f decreases. In near IR, the photonic band structure exhibits two-gap or four gap structure, depending on the size of spatial periodicity. A larger periodicity will yield more gaps in the band diagram. The effects of doping concentration have been shown. That is, it can not only enhance the band gap but shift the position of band gap. Finally, the influence of filling factor in the band gap structure is also demonstrated.

ACKNOWLEDGMENT

REFERENCES

1. John, S., "Electromagnetic absorption in a disordered medium near a photon mobility edge," *Phys. Rev. Lett.*, Vol. 53, 2169–2173, 1984.

2. John, S., "Strong localization of photons in certain disordered lattices," *Phys. Rev. Lett.*, Vol. 58, 2486–2489, 1987.

3. Yablonovitch, E., "Inhibited spontaneous emission in solid state physics and electronics," *Phys. Rev. Lett.*, Vol. 58, 2059–2062, 1987.

4. Li, H. and X. Yang, "Larger absolute band gaps in two-dimensional photonic crystals fabricated by a three-order-effect method," *Progress In Electromagnetics Research*, Vol. 108, 385–400, 2010.

5. Wu, C.-J. and Z.-H. Wang, "Properties of defect modes in one-dimensional photonic crystals," *Progress In Electromagnetics Research*, Vol. 103, 169–184, 2010.

6. Wu, C.-J., J.-J. Liao, and T.-W. Chang, "Tunable multilayer Fabry-Perot resonator using electro-optical defect layer," *Journal of Electromagnetic Waves and Applications*, Vol. 24, No. 4, 531–542, 2010.

7. Rahimi, H, A. Namdar, S. Roshan Entezar, and H. Tajalli, "Photonic transmission spectra in one-dimensional fibonacci multilayer structures containing single-negative metamaterials," *Progress In Electromagnetics Research*, Vol. 102, 15–30, 2010.

8. Chen, D., M.-L. Vincent Tse, and H.-Y. Tam, "Optical properties of photonic crystal fibers with a fiber core of arrays of subwavelength circular air holes: Birefringence and dispersion," *Progress In Electromagnetics Research*, Vol. 105, 193–212, 2010.

9. Nozhat, N. and N. Granpayeh, "Specialty fibers designed by photonic crystals," *Progress In Electromagnetics Research*, Vol. 99, 225–244, 2009.

10. Shi, Y., "A compact polarization beam splitter based on a multimode photonic crystal waveguide with an internal photonic crystal section," *Progress In Electromagnetics Research*, Vol. 103, 393–401, 2010.

11. Bermann, O. L., Y. E. Lozovik, S. L. Eiderman, and R. D. Coalson, "Superconducting photonic crystals," *Phys. Rev. B*, Vol. 74, 092505, 2006.

12. Takeda, H. and K. Yoshino, "Tunable photonic band schemes in two-dimensional photonic crystals composed of copper oxide high-temperature superconductors," *Phys. Rev. B*, Vol. 67, 245109, 2005.

13. Wu, C.-J., M.-S. Chen, and T.-J. Yang "Photonic band structure for a superconducting-dielectric superlattice," *Physica C*, Vol. 432, 133–139, 2005.

14. Wu, C.-J., "Transmission and reflection in a periodic superconductor/dielectric film multilayer structure," *Journal of Electromagnetic Waves and Applications*, Vol. 19, No. 15, 1991–1996, 2005.

15. Wu, C.-J., C.-L. Liu, and W.-K. Kuo "Analysis of thickness-dependent optical properties in a one-dimensional superconducting photonic crystal," *Journal of Electromagnetic Waves and Applications*, Vol. 23, No. 8–9, 1113–1122, 2009.

16. Lin, W.-H., C.-J. Wu, T.-J. Yang, and S.-J. Chang, "Terahertz multichanneled filter in a superconducting photonic crystal," *Optics Express*, Vol. 18, 27155–27166, 2010.

17. Anlage, S. M., "The physics and applications of superconducting metamaterials," *J. Optics*, Vol. 13, 024001, 2011.

18. Lyubchanskii, I. L., N. N. Dadoenkova, A. E. Zabolotin, Y. P. Lee, and T. Rasing, "A one-dimensional photonic crystal with a superconducting defect layer," *J. Optics A: Pure Appl. Opt.*, Vol. 11, 114014, 2009.

19. Choudhury, P. K. and W. K. Soon, "TE mode propagation through tapered core liquid crystal optical fibers," *Progress In Electromagnetics Research*, Vol. 104, 449–463, 2010.

20. McPhail, D., M. Straub, and M. Gu, "Optical tuning of three-dimensional photonic crystals fabricated by femtosecond direct writing," *Appl. Phys. Lett.*, Vol. 87, 091117, 2005.

21. Halevi, P., J. A. Reyes-Avendano, and J. A. Reyes-Cervantes, "Electrically tuned phase transition and band structure in a liquid-crystal-infilled photonic crystal," *Phys. Rev. E*, Vol. 73, R040701, 2006.

22. Qi, L.-M. and Z. Yang, "Modified plane wave method analysis of dielectric plasma photonic crystal," *Progress In Electromagnetics Research*, Vol. 91, 319–332, 2009.

23. Tian, H. and J. Zi, "One-dimensional tunable photonic crystals

by means of external magnetic fields," *Optics Commun.*, Vol. 252, 321–328, 2005.

24. Sabah, C. and S. Uckun, "Multilayer system of lorentz/drude type metamaterials with dielectric slabs and its application to electromagnetic filters," *Progress In Electromagnetics Research*, Vol. 91, 349–364, 2009.

25. Inoue, M., R. Fujikawa, A. Baryshev, A. Khanikaev, P. B. Lim, H. Uchida, O. Aktsipetrov, A. Fedyanin, T. Murzina, and A. Granovsky, "Magnetophotonic crystals," *J. Phys. D: Appl. Phys.*, Vol. 39, R151–R161, 2006.

26. Lyubchanskii, I. L., N. N. Dadoenkova, M. I. Lyubchanskii, E. A. Shapovalov, and T. Rasing, "Magnetic photonic crystals," *J. Phys. D:Appl. Phys.*, Vol. 36, R227–R287, 2003.

27. Fu, X., C. Cui, and S. C. Chan, "Optically injected semiconductor laser for photonic microwave frequency mixing in radio-over-fiber," *Journal of Electromagnetic Waves and Applications*, Vol. 24, No. 7, 849–960, 2010.

28. Mustafa, F. and A. M. Hashim, "Properties of electromagnetic fields and effective permittivity excited by drifting plasma waves in semiconductor-insulator interface structure and equivalent transmission line technique for multi-layered structure," *Progress In Electromagnetics Research*, Vol. 104, 403–425, 2010.

29. Figotin, F., Y. A. Godin, and I. Vitebsky, "Two-dimensional tunable photonic crystals," *Phys. Rev. B*, Vol. 57, 2841–2848, 1998.

30. Golosovsky, M., Y. Saado, and D. Davidov, "Self-assembly of floating magnetic particles into ordered structures: A promising route for the fabrication of tunable photonic band gap materials," *Appl. Phys. Lett.*, Vol. 75, 4168–4170, 1999.

31. Kee, C.-S., J. E. Kim, H. Y. Park, and H. Lim, "Two-dimensional tunable magnetic photonic crystals," *Phys. Rev. B*, Vol. 61, 15523–15525, 2000.

32. Galindo-Linares, E., P. Halevi, and A. S. Sanchez, "Tuning of one-dimensional Si/SiO_2 photonic crystals at the wavelength of 1.54 mm," *Solid State Commun.*, Vol. 142, 67–70, 2007.

33. Yeh, P., *Optical Waves in Layered Media*, John Wiley & Sons, Singapore, 1991.

34. Kumar, V., K. S. Singh, and S. P. Ojha, "Enhanced omni-directional reflection frequency range in Si-based one dimensional photonic crystal with defect," *Optik*, 2010.